Synergistic effect of CdS Nanoflower for removal of highly toxic aqueous Cr(VI)

Anurag Roy,* Sasireka Velusamy, Tapas K Mallick, Senthilarasu Sundaram*

Environment and Sustainability Institute, University of Exeter, Penryn Campus, Cornwall TR10 9FE, U.K.

*Corresponding Author

Email: A.Roy30@exeter.ac.uk; s.sundaram@exeter.ac.uk;

Phone: 01326 259486

A B S T R A C T

Thiourea assisted hydrothermal preparation of CdS nanoflowers (NFs) synthesis and its efficient application to remove toxic Cr (VI) in aqueous solution has been reported in this article. The NFs show synergistic behaviour *via* photo-catalytic reduction and adsorption to remove the toxic Cr (VI) and reduce to non-toxic Cr (III) ionic state in the aqueous solution at the room temperature (25 °C). The adsorption of Cr (VI) from the aqueous solution stable time was observed ~120 min at the pH of 2 with an adsorption efficiency of 92%. Various adsorptions of kinetic and isothermal models have been applied to understand the adsorption mechanism. The results show that the adsorption occurs based on the assumption of the pseudo-second-order kinetic model by chemisorption and mechanism of internal diffusion. The equilibrium adsorption isotherm revealed that the Langmuir model better describes the adsorption process. These results confirm the possibility of toxic Cr (VI) removal in water remediation without employing any costly noble metal based catalyst.

Keywords: Cr (VI), Toxic, Waste Water, Synergetic, Kinetics

1. Introduction

The presence of chromium (Cr) in industrial effluents have adverse effects to living species as hexavalent chromium, Cr (VI) is highly toxic due to its ability to generate reactive oxygen species in cells **[1]**. Even though Cr is known to exhibit several oxidation states, only Cr (III) and Cr(VI) are of environmental importance. In the aqueous environment, Cr(III) may hydrolyze into several species including $Cr(OH)^{2+}$, $Cr(OH)_2^{+}$, $Cr(OH)_4$, neutral species $Cr(OH)_3$ and polynuclear species $Cr_2(OH)_2$ and $Cr_3(OH)4^{5+}$. The trivalent state of chromium, on the other hand, is significantly less toxic and also serves as an essential

element in trace amounts. When industries such as electroplating, tannery, dyeing and others release their effluents into water bodies, hexavalent chromium enters the food chain and, consequently, reaches humans in a biomagnified form. Cr (VI) is dangerous to health when the limit (0.05 $mg.L^{-1}$) exceeds in potable water **[2-4]**. Various physio- chemical methods are available for removal of Cr (VI) from aqueous solutions, such as chemical precipitation, filtration, chemical oxidisation and reduction, adsorption, reverse osmosis, evaporation techniques, electrochemical and ion exchange, however these methods have some limitations such as membrane fouling, high energy requirement, high cost and incomplete removal of metals and so on **[5, 6]**. Among these conventional methods adsorptions have more advantage than other methods due to its cost effectiveness, regeneration ability and applicable for large scale applications. Cadmium sulfide (CdS) has attracted in the field of photocatalytic degradation, water splitting and solar energy conversion owing to its narrow band gap (2.5 eV), which enables it to absorb and make effective use of light. CdS has exhibited its adsorption properties in many others reports as well **[7]**. In this report, CdS exhibited a synergistic effect of adsorption and photo-catalytic reduction of Cr (VI) in aqueous solution. The photocatalytic reduction of Cr(VI) to Cr (III) and adsorption process of Cr (VI) have indicated that these processes are pH-dependent where maximum Cr (VI) removal occurring in acidic conditions depending on the surface charge of the adsorbent.

2. Materials and Method

The CdS Nanoflowers has been synthesized by a modified method of thirourea assisted hydrothermal route **[8]**. The details have been mentioned in the Supplementary Information (SI). Material characterization and study of Cr (VI) Removal is illustrated in the SI.

3. Results and Discussions

The XRD pattern of the synthesized CdS sample is shown in Fig. S1(a), SI. All of the diffraction peaks could be indexed to those of hexagonal wurtzite CdS (JCPDS No. 80-0006). Raman spectra in Fig. S1(b) shows that the characteristics Raman lines of CdS at 298 and 593 cm^{-1} **[9]**.

The UV-vis absorption spectrum of CdS NFs exhibited an absorption edge ($\lambda_{abs.}$) at ~ 483 nm (Fig. S1 c, SI). Besides, the green emission at 536 nm ($\lambda_{emi.}$) was observed on excitation at 390 nm as shown in the photoluminescence spectra of aqueous solution of the CdS

sample in Fig.S1 c, SI. Fig. 1a shows the FESEM microstructural images flower-like architecture termed as nanoflowers (NFs) composed of branches in different directions. The homogeneous distribution with distinct colour contrast of elements as Cd and S are very clear from the elemental mapping diagram (Fig. 1b). The growth of nano-crystallites proceeded anisotropically along the [001] direction with a high growth rate, resulting in the formation of flower-like CdS structure **[8]**. During the addition of CTAB, the Cd atoms could be coordinated with more thiourea species, making the branch growth of flower-like CdS were largely restrict (Fig. 1c)

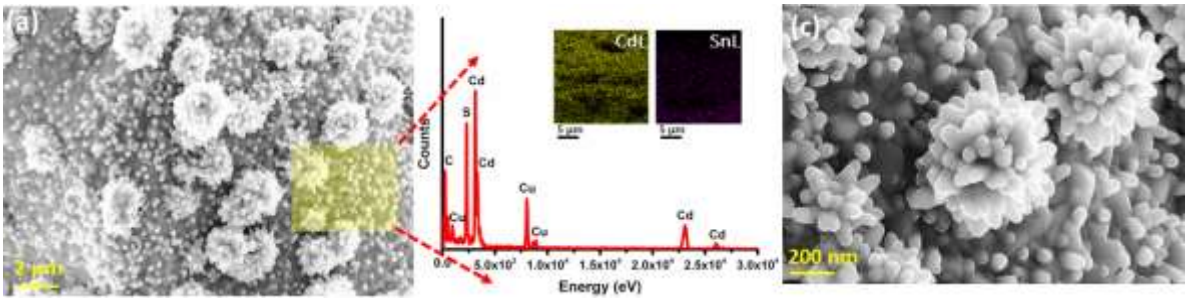

Fig.1 FESEM microstructural image at (a) higher magnification along with corresponding elemental analysis and (b) lower magnification of CdS Nanoflowers, respectively.

The reduction of Cr (VI) was found to be highly pH dependent. It follows half reaction as mentioned below (Equation 1):

$$Cr_2O_7^{2-} + 14\,H^+ + 6e^- \longrightarrow 2\,Cr^{3+} + 7\,H_2O, \quad E^0(v) = +1.33 \qquad (1)$$

Potassium dichromate ($K_2Cr_2O_7$) was taken as a representative molecule for Cr (VI). $K_2Cr_2O_7$ absorbs UV-visible light in the range of 250-500 nm as a result of the ligand-to-metal charge transfer transition (Fig. 2a). However, in presence of CdS NF, the absorption bands of dichromate (Fig. 2a) decreases rapidly and almost disappears within ~120 min of reaction at a pH 2. This indicates complete adsorption of the Cr (VI). Besides, the colour of the solution changes from deep yellow to almost colourless, confirming the complete reduction of Cr (VI) to Cr (III). Appearance of Cr (III) was further confirmed by the extrapolation of Cr (VI) adsorption plot at ~563 nm as shown in Fig. 2b. The presence of Cr (III) in the colourless solution was also confirmed by treating it with excess NaOH solution that gives rise to a green solution resulting from the formation of hexahydroxochromate (III) **[10]**. In order to establish the time-dependent adsorption, the adsorption capacity of dichromate solution on CdS NFs as a function of contact time was evaluated experimentally. The initial faster

adsorption is caused by surface electrostatic attraction on the CdS NFs surface because of the existence of a large number of adsorption sites and saturated the adsorption capacity by 200 min. (Fig. 3c). The adsorption and photo-catalytic reduction process is strictly depends on the pH of the solution as monitored by calculating the adsorption efficiency as shown in Fig. 2d. Fig. 2e shows the digital image of the aqueous solution of the yellow dichromate solution which turns almost colourless during interaction with CdS after 120 min and monitored until 200 min.

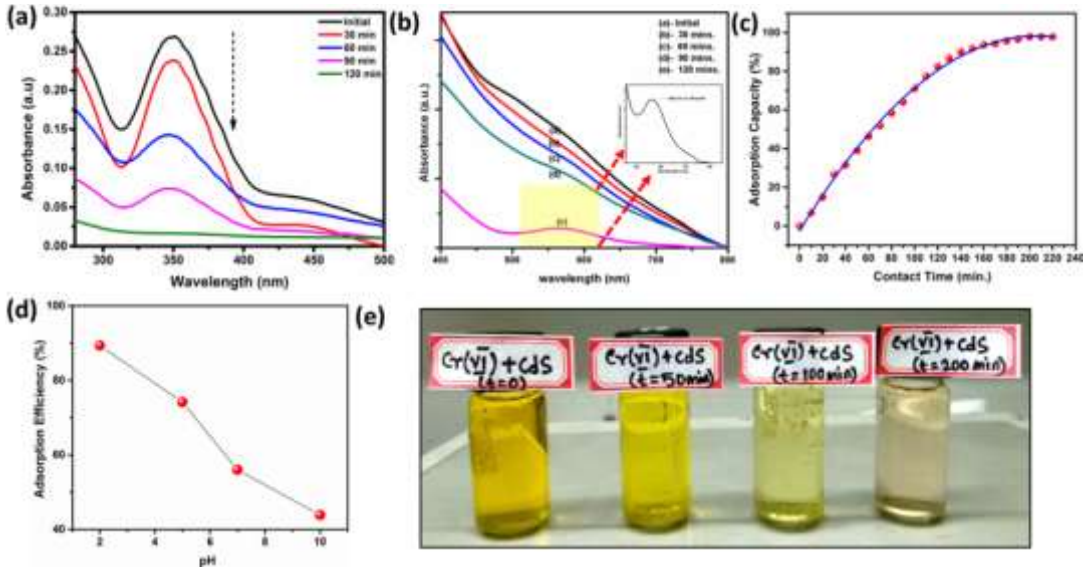

Fig. 2 (a) and (b) UV-visible spectral evolution with time during the reduction of $Cr_2O_7^{2-}$ by CdS Nanoflowers at 25 °C, (c) plot of Cr (VI) adsorption capacity against contact time, (d) plot of pH dependent adsorption efficiency of Cr (VI) and (e) digital image of aqueous solution of the yellow dichromate solution which turns almost colourless during interaction with CdS.

In order to investigate the adsorption mechanism, the pseudo first- order and pseudo-second-order model were verified **[11]**. The pseudo-first-order model describes the adsorption of a solute from an aqueous solution (Equation 2). The pseudo-first-order model is represented below:

$$\log(q_e - q_t) = \log q_e - \frac{k_1}{2.303}\, t \qquad (2)$$

Where, q_e and qt ($mg.g^{-1}$) are the amount of Cr (VI) at equilibrium and time t (min), respectively, and k_1 (min^{-1}) is the pseudo first- order rate constant.

The pseudo-second-order model is based on the adsorption capacity of the solid phase (3). The model is expressed as:

$$\frac{t}{q_t} = \frac{1}{k_2 q_e^2} + \frac{t}{q_e} \quad (3)$$

Fig. 3a,b shows a plot of the pseudo-first-order and pseudo-second-order kinetic models for Cr (VI) adsorption on CdS. Table 1 gives the rate constants of the two models with their correlation coefficients. The pseudo-second-order is more suitable for describing the adsorption process, as evident from the correlation coefficient.

Langmuir and Freundlich adsorption isotherm models were employed for the adsorption analysis **[12]**. The Freundlich isotherm model was employed to describe heterogeneous systems (Fig. 3c). The mathematical expression (Equation 4) of the Freundlich isotherm model is,

$$\ln q_e = \ln k_F + b_F \ln C_e \quad (4)$$

where, k_F (mg.g^{-1}) is the Freundlich constant, b_F (g.mL^{-1}) is a constant depicting the adsorption intensity.

The Langmuir isotherm model was used to describe homogeneous systems (Fig. 3d). Such a model was exploited to represent the relationship between the amount of Cr (VI) adsorbed at equilibrium (q_e, mg.g^{-1}) and the equilibrium solute concentration (C_e, mg L^{-1}), while monolayer formation occurs on adsorbate surface sites. The equation is as follows (Equation 5):

$$\frac{C_e}{q_e} = \frac{C_e}{q_{max}} + \frac{1}{q_{max} k_L} \quad (5)$$

where, q_{max} (mg.g^{-1}) is the maximum adsorption capacity of the adsorbent and K_L (L.mg^{-1}) is the Langmuir adsorption constant. The obtained parameters derived from different kinetics models and isotherms as shown in Fig. 3 are tabulated in Table 1.

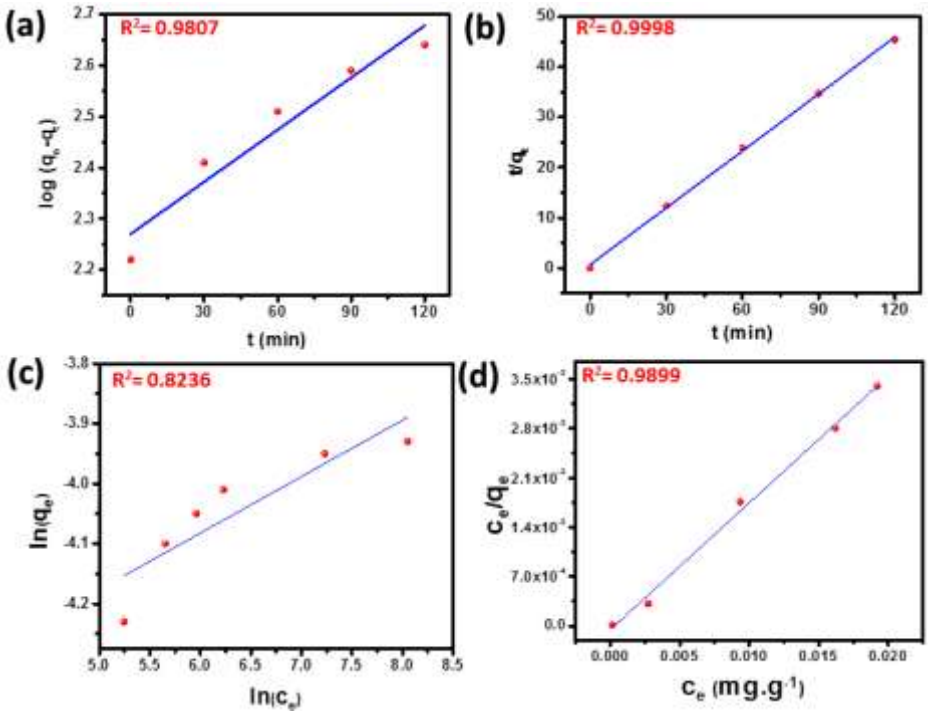

Fig. 3 (a) Pseudo-first-order (b) pseudo-second-order kinetic plot, (c) Freundlich and (d) Langmuir adsorption isotherm plot for the adsorption of Cr (VI) on CdS Nanoflowers, respectively.

Table. 1 The obtained parameters for different kinetic and adsorption isotherm model for Cr(VI) adsorption on CdS NFs, respectively

Pseudo-first-order Kinetic Model				**Pseudo-second-order Kinetic Model**		
$q_{e(exp.)}$ (mg.g^{-1})	k_1	$q_{e(cal.)}$ (mg.g^{-1})	R^2	k_2 (g.min^{-1}.mg^{-1})	$q_{e(cal.)}$ (mg.g^{-1})	R^2
440.83	1.2 x 10^{-2}	396.47	0.9807	1.2 x 10^{-4}	398.47	0.9998
Langmuir Isotherm				**Freundlich Isotherm**		
q_{max} (mg.g^{-1})	K_L (g.ml^{-1})	R^2		K_F (mg.g^{-1})	b_F (g.ml^{-1})	R^2
403.23	53.54	0.9899		123.72	0.9678	0.8236

As evident in Fig. 3c,d, the Langmuir isotherm model coincides very well with the experimental data; better than the Freundlich isotherm model. This suggests that active sites are homogeneously distributed on the surface of the adsorbent and the adsorption process is monolayer coverage of the Cr (VI) solution on the surface of the CdS **[13, 14]**.

Conclusions

In summary, CdS nanoflowers (NFs) have been successfully synthesized using hydrothermal technique and characterized by various physico-chemical techniques. These NFs are further

introduced in waste water treatment for removal of highly toxic Cr (VI) ion. It is observed that the CdS NFs show synergistic behaviour *via* photo-catalytic reduction and adsorption to remove the toxic Cr (VI) and reduced to non-toxic Cr (III) ionic state in the aqueous solution. The maximum adsorption capacity of the studied adsorbents for Cr was observed at a pH of 2. For the adsorption of Cr (VI) from the aqueous solution stable time was found 120 min. Experimental results were more fitted to the data attained from Langmuir adsorption isotherm model at different level of temperatures. Pseudo-second-order kinetic model was best fitted for Cr (VI) adsorption. Therefore, we believe that this new composite material will find applications in the water remediation and is expected to replace Pd-based expensive materials in many other systems.

Acknowledgements

S.V would like to acknowledge the College of Engineering, Mathematics, and Physical Sciences, University of Exeter for the PhD fellowship. This work has been conducted as part of the research project 'Joint UK-India Clean Energy Centre (JUICE)' which is funded by the RCUK's Energy Programme (contract no: EP/P003605/1). The projects funders were not directly involved in the writing of this article.

Notes

The authors declare no competing financial interest.

References

[1] M. Owlad et. al., Water Air Soil Pollut. 200 (2009) 59-77

[2] S. Mitra et. al., Nanotechnol. Environ. Eng. 2:11 (2017) 1-14.

[3] F. Fu et. al., J. Environ. Management 92 (2011) 407-418

[4] M. Shahid et. al., Chemosphere 178 (2017) 513-533

[5] V.E.Pakade et.al., RSC Adv. 9 (2019) 26142-26164

[6] H.A. Maitlo et. al., Environ. Int. 130 (2019) 104748

[7] A. Roy et. al., Beilstein J. Nanotechnol. 8 (2017) 210-221

[8] X. Yang et. al., New J. Chem. 43 (2019) 10126-10133

[9] P. Kumar et. al., Nanoscale res. Lett. 7:584 (2012) 1-7

[10] K. Bhowmik et. al., Langmuir 30 (2014) 3209-3216

[11] H. Liu et. al., Sci. Rep. 9:3663 (2019) 1-12

[12] W-R Lim et. al., Sci. Rep. 9:13598 (2019) 1-10

[13] X. Liu et. al., Chem. Commun. 47 (2011) 11984-11986

[14] L. Zhang et. al., J Colloid Interf. Sci. 514 (2018) 396-406